Chemical modification of PDMS surface without impacting the viscoelasticity: Model systems for a better understanding of elastomer/elastomer adhesion and friction

Mohammed Dirany[a], Laëtitia Dies[b], Frédéric Restagno[b], Liliane Léger[b], Christophe Poulard[b], Guillaume Miquelard-Garnier[a,*]

[a] Laboratoire PIMM, UMR 8006, ENSAM, CNAM, CNRS, 151 boulevard de l'Hôpital, 75013 Paris, France
[b] Laboratoire de Physique des Solides, UMR 8502, Université Paris Sud, CNRS, bâtiment 510, 91405 Orsay Cedex, France

HIGHLIGHTS

- Poly(dimethylsiloxane) surfaces were modified with poly(ethylene glycol).
- Surface modification via hydrosilylation has no impact on viscoelastic properties.
- Modified surfaces exhibit lower contact angle and higher surface energy.

GRAPHICAL ABSTRACT

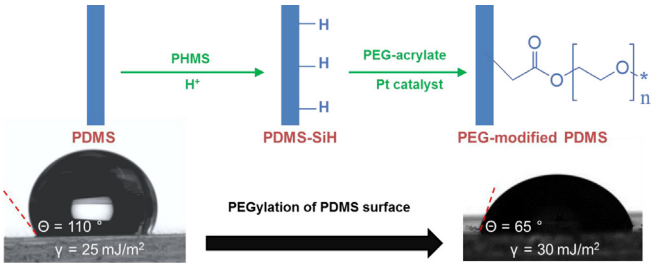

ARTICLE INFO

Keywords:
Poly(dimethylsiloxane) elastomers
Surface modification
Hydrosilylation
Contact angle
Surface energy
Viscoelastic properties

ABSTRACT

The influence of both viscoelastic and interfacial parameters on the surface properties of elastomers is difficult to study. Here, we describe a simple route to achieve surface modification of PDMS without impacting the viscoelastic properties of the bulk. PEG modified PDMS surfaces were synthesized by two step surface modification based on hydrosilylation. The covalent grafting of PEG on the surface has been evidenced by AFM and ATR-FTIR, and its effect on the hydrophilicity characterized by static and dynamic contact angle. The static water contact angle of the PEG-modified PDMS decreases from 110° (for unmodified PDMS) to 65°. Dynamic contact angles also show a significant decrease in both advancing and receding contact angles, along with a significant increase in the contact angle hysteresis, which can be related to an increase in the surface energy as estimated by JKR measurements. The viscoelastic properties of modified PDMS are found to be quantitatively comparable to those of the unmodified PDMS. This simple method is an efficient way to prepare model materials which can be used to get a better understanding of the exact contribution of the surface chemistry on surface properties of elastomers.

1. Introduction

The frictional and adhesive behaviors of elastomers depend on the viscoelastic properties but also on interfacial parameters such as the surface chemistry and the surface topography of the two materials in contact [1–5]. The role of chemical interactions at the interface [6] and surface patterning [7–11] as well as viscoelasticity effects [12,13] on adhesion, friction, and also on other surface properties such as wetting, has thus started to be investigated extensively over the last years, but mostly independently from each other. However a real deep understanding of the coupling between these properties remains a challenge, and in consequence there is still a lack of prediction of the global effect of such properties.

* Corresponding author. Tel.: +33 01 71 93 65 72.
E-mail address: guillaume.miquelard_garnier@cnam.fr (G. Miquelard-Garnier).

To identify the incidence of patterning on wetting, adhesion, and friction mechanisms, commercial polydimethylsiloxane (PDMS)-based elastomers have often been chosen as candidates as they have good mechanical properties, good thermal and chemical stability, transparency, and can be easily fabricated and patterned with good reproducibility. These features make these materials perfectly suited for applications in microfluidic or transfer printing. However, PDMS is rather chemically stable and has a low surface free energy (measured between 21 and 25 mJ/m^2) [14]. Moreover, these materials lack reactive surface groups, and may present low-molecular-weight mobile components having a high tendency to migrate to the PDMS surface from the bulk. This results in relatively poor intrinsic adhesive properties for these materials.

On the other hand, chemical modification of PDMS interface can drastically alter its frictional, adhesive and wetting properties but will also, in general, affect its mechanical properties. Indeed, developing a simple route to change the chemical properties of PDMS surfaces only, without impacting the bulk modulus (or creating, from a mechanical point of view, a bilayer system), is a challenging task which would prove useful to design model systems for a better understanding of the exact contribution of the surface chemistry on surface properties (adhesion, friction and wetting) of elastomers.

To modify the properties of PDMS surfaces and confer hydrophilicity to PDMS surfaces, various surface modification methods have been explored. One of the easiest means for generating the hydrophilic PDMS surface is its exposure to an air or oxygen plasma treatment [15,16]. However, this treatment leads to the formation of a stiff SiOH layer at the surface, which will then make the physical analysis of surface properties difficult and can lead to uncontrolled wrinkling and associated phenomena like surface cracks and grooves [17]. Furthermore, the result of this kind of treatment is temporary, and the surface will usually recover its hydrophobicity within a few hours due to low molecular weight chains diffusing to the surface and rearrangement of polymer chains near the interface [18,19]. Vickers et al. [20] used a two-step process involving solvent extraction of the oligomers followed by oxidation as one approach to solve this problem, making oxidized PDMS surfaces stable for at least 7 days in air but this kind of treatment still generates a stiff SiO_2 layer.

Several other PDMS hydrophilic surface modification strategies have been explored, such as UV treatment [21,22], chemical vapor deposition [23], layer-by-layer (LBL) deposition [24,25], sol–gel coatings [26], silanization [27], dynamic modification with surfactants [28], and protein adsorption [29], but all result in the formation of what can be seen as a bilayer system unstable over time.

Another approach for altering the properties of PDMS consists in predoping PDMS with chemicals (such as acrylic acid and undecylenic acid) [30] that will infuse in the matrix. However, by doing so, the chemical groups can perturb the crosslinking reaction and induce a significant change in the bulk mechanical properties of the elastomer. This approach depends also on the applicability of the chemical to be mixed with PDMS and the weight ratio of the added chemical. Seo and Lee [31] improved the wettability of PDMS by directly incorporating a nonionic surfactant into the PDMS. The concentration of the surfactant at the surface could then be changed by surface migration upon exposure to various solvents. Surface-initiated ATRP has been also used. Typically it involves creation of reactive sites on the PDMS surface followed by covalent linkage of a preformed polymer or more commonly a monomer that can then be used as the initiation site for a polymeric chain [32]. PEG was also tethered onto PDMS surface by using a swelling–deswelling method with block copolymers comprising PEG and PDMS segments [33]. All these treatments are long, complicated and dramatically alter the bulk and mechanical PDMS properties (often by a factor of 2 or more on the modulus when compared to unmodified PDMS).

An easier path consists in coating PDMS surface with hydrophilic polymers such as poly(ethylene glycol) (PEG) and its derivatives. Several techniques have been proposed to achieve this grafting. Star shaped PEG was grafted on PDMS functionalized using ammonia plasma treatment [34]. Simpler, Brook et al. developed a route using poly(ethylene glycol) monoallylether [35]. This method is a two-step surface modification process. Since PDMS does not have appropriate functional groups on the surface available to react with PEG, modification is necessary to introduce first active sites for subsequent functionalization. PDMS is initially functionalized with SiH groups under acid catalysis to give PDMS–SiH, followed by a platinum catalyzed hydrosilylation reaction with PEG. This is an addition reaction between SiH and allyl groups of PEG to create SiC bonds, and it is a method to replace the methyl groups on PDMS with PEG. A similar reaction was used by Iwasaki et al. [36] to graft triblock copolymers composed of poly(2-methacryloyloxyethyl phosphorylcholine) (PMPC) and poly(vinylmethyl siloxane-co-dimethylsiloxane) onto the PDMS surface.

Inspired by this two-step strategy, we chose poly(ethylene glycol) methyl ether acrylate (PEG-acrylate) to modify PDMS surfaces through covalent bonding of PEG-acrylate chains on PDMS surfaces. We chose poly(ethylene glycol) acrylate (PEG-acrylate) because of three reasons: (1) this molecule has a terminating acrylic group (2) it is inexpensive and commercially available from common chemical companies with various molar masses and (3) the lower molar masses are liquid at room temperature, making it easy to react with PDMS disks of relatively large proportions. Moreover, the layer formed, being only a few monomers long, could be added on flat or patterned surfaces, and has the potential to be “invisible” in terms of mechanical properties.

The changes of PDMS surface properties during and after PEGylation are analyzed at different reaction times using contact angle measurements, AFM and ATR-FTIR study. The effects of this surface modification in terms of hydrophobicity were studied using both static and dynamic contact angles measurements. JKR technique was also used to determine the surface free energy and was coupled with rheological experiments to determine and compare Young’s modulus and loss modulus of modified and unmodified PDMS.

2. Materials and methods

2.1. Materials

Sylgard 184, a PDMS kit containing two parts, a liquid silicon rubber base and a curing agent, was purchased from Dow-Corning. Polyhydromethylsiloxane (PHMS), trifluoromethanesulfonic acid (CF_3SO_3H) were purchased from Merck. Karstedt’s platinum catalyst (platinum(0)–1,3-divinyl-1,1,3,3-tetramethyldisiloxane complex, soln. in vinyl terminated polydimethylsiloxane), diethylene glycol dimethyl ether (99%), anhydrous methanol, hexane and toluene were purchased from Alfa Aesar and used as received. Poly(ethylene glycol) methyl ether acrylate (PEG-acrylate, M_n = 480 g/mol given by the supplier), a viscous liquid, was obtained from Sigma Aldrich.

2.2. Methods

2.2.1. Preparation and surface modification of PDMS films

2.2.1.1. PDMS substrates. PDMS samples used in the present study for the surface modifications experiments were prepared using the Sylgard 184 silicone elastomer kit by the classical procedure,

consisting in mixing the elastomer base (vinyl-terminated PDMS linear chains) with the curing reagent (short chains presenting Si—H functions to react with the vinyl groups) in a 10:1 (w/w) ratio (unless otherwise specified) followed by degassing in vacuum for about 15 min to remove the bubbles formed during mixing. The mixture was poured into a Petri dish and cured at 70 °C for 17 h in an oven. The resulting film, about 1 mm thick (1.5 for rheological measurements), was cut into 2 cm (2.6 for rheological measurements) diameter discs for chemical modification and further analysis.

2.2.1.2. Surface modification of PDMS substrates. Fig. 1 illustrates the reaction scheme of the surface modification of PDMS.

The incorporation of SiH groups on the PDMS surfaces involves exchanging Me_2SiO of PDMS with HMeSiO of PHMS using acid catalysis. This leads to PDMS with a high concentration of SiH groups on its surface (see Fig. 1). To introduce SiH groups into the PDMS surface (PDMS–SiH), each PDMS disk was immersed in 3 mL of polyhydromethylsiloxane (PHMS) with 5 mL of anhydrous methanol (e.g. PHMS is in excess). 50 μL of trifluoromethanesulfonic acid was added as a catalyst and the system was set for 30 min at room temperature. One can notice that lower concentrations of trifluoromethanesulfonic acid are also effective, but require longer reaction times. Surfaces were then rinsed sequentially in 10 mL methanol, 10 mL hexane and 10 mL methanol to remove residual reactants, and dried under vacuum for 8 h. Finally, samples were stored under anhydrous conditions in a desiccator to prevent loss of SiH groups. During the surface functionalization, two competing reactions occur: the first involves surface monomer exchange and the second degradation (breaking of the covalent network due to the presence of the acid) of PDMS. The efficiency of each reaction depends on various factors such acid catalyst concentration and reaction times. Increased reaction times lead to increase SiH groups at the surface of PDMS for about 30 min of reaction time. Longer reaction times and higher concentrations in acid catalyst lead to depolymerization process of the PDMS [36–38].

In order to prepare the PEG modified surfaces, PDMS–SiH disks (4 maximum) were introduced into 20 mL a mixture of PEG-acrylate and diethylene-glycol dimethyl ether (1:3, v/v). In these proportions, PEG-acrylate is in large excess compared to SiH even assuming total functionalization of the surfaces. Catalytic amount (one drop) of Karstedt's catalyst (platinum–divinyltetramethyldisiloxane complex) was added to the reaction solution and the mixture was stirred for different reaction times (between 4 and 72 h) at 70 °C. It is worth noting that the choice of solvent in particular is critical in the two steps of the process. It is necessary to use a solvent that does not react with the highly reactive hydrosilane groups. Solvents that swell the silicone, such as hexane, toluene, would also lead to Si—H incorporation throughout the elastomer and internal hydrosilylation.

To characterize the bonding between the PEG-acrylate and PDMS after modification, any free PEG-acrylate unreacted with PDMS needs to be removed from the PDMS discs. Acetone is a good solvent for PEG-acrylate while being a poor solvent for PDMS. Washing PDMS discs with acetone can completely extract unreacted PEG-acrylate from the bulk PDMS. PDMS pieces were characterized after this extraction process and drying under vacuum at room temperature overnight.

2.2.2. ATR-FTIR spectroscopy

Fourier transform infrared spectroscopy in attenuated total reflectance (ATR-FTIR) mode was used to analyze the effects of PEGylation on the surface chemistry of PDMS. ATR-FTIR spectroscopy measurements were carried out on a Perkin Elmer Frontier spectrometer. The data were collected using a diamond ATR crystal plate from 450 to 4000 cm^{-1}, with resolution of 4 cm^{-1}, and analyzed using Spectrum software.

The depth of penetration, d_p is given by (Eq. (1)):

$$d_p = \frac{\lambda}{2\pi(n_1^2(\sin\theta)^2 - n_2^2)^{1/2}} \quad (1)$$

where λ is the wavelength of light, θ is the angle of incidence of the IR beam relative to the perpendicular of the crystal surface, n_1 is the refractive index of the diamond (2.4 in this range of wavelengths) and n_2 is the refractive index of the PDMS (1.4 as given by Dow-Corning).

The depth of penetration is then ~1 μm at 2000 cm^{-1}.

2.2.3. Surface characterization by atomic force microscopy (AFM)

AFM images were obtained in tapping mode with a Multimode microscope and a Nanoscope V controller (Veeco) using the Nanoscope V7.2 software, operated under ambient atmosphere. The tips (Tap300-G model; spring constant 40 N/m, oscillation frequency 300 kHz, tip radius < 10 nm) were obtained from BudgetSensors. The images were recorded at a scan rate of 1 Hz. The root-mean square (RMS) roughness (standard deviations of the height value within a given image) was calculated with the software, using the following formula (Eq. (2)):

$$R_q = \sqrt{\frac{1}{N}\sum_{i=1}^{N}(Z_i - Z_{ave})^2} \quad (2)$$

where Z_{ave} is the average Z value within the given image, Z_i is the current Z value and N is the number of points within a given image.

2.2.4. Rheological measurements

The changes in the viscoelastic properties of the PDMS due to the surface modification were assessed by comparing unmodified and modified PDMS using an Anton Paar rheometer MCR502. Crosslinked PDMS Sylgard 184 has a tendency to slip under the plates of the rheometer. To the best of our knowledge, the only extensive study of the viscoelastic properties of this material [39] has been performed by having the samples crosslink directly between the plates to ensure good adhesion between the sample and the rheometer. In our case, this method was not possible, since chemical modification was made after the crosslinking. In consequence, we used a grooved plate-plate geometry (25 mm) to test our samples (1.5 mm thick, 2.6 mm in diameter). When the sample and the plates are in contact with no normal force, the measured G' for the unmodified PDMS can be as much as 10× lower than expected values (estimated from independent measurements of the Young's modulus E, using JKR or tensile tests), which was attributed to slippage. In consequence, to prevent this, an initial compression between 25% and 30% was applied to the sample. In this deformation range for uniaxial compression (or around 20% in biaxial extension), PDMS Sylgard 184 still displays a linear elastic behavior [40].

To measure G' and G'', deformation sweep tests at constant frequency (1 Hz) and frequency sweep tests at constant deformation (0.1%) were then performed at room temperature. Other frequencies (0.1 Hz) and deformations (1%) were tested to ensure the results were within the linear regime. Only the deformation sweep tests will be presented in this study.

The reference material (1:10 PDMS Sylgard 184 cured 17 h at 70 °C) was measured as made from 5 different initial mixtures. For 2 of these mixtures, 2 disks samples cut from different places of the global samples were also tested.

For the other materials, the results were averaged over two samples from the same batch, unless otherwise specified.

The compliance of the rheometer was not taken into account in this study. However, estimates made using McKenna et al. approach [41,42] and assuming the compliance of the Anton Paar rheometer is similar to that of the ARES and the RDA II from TA Instruments

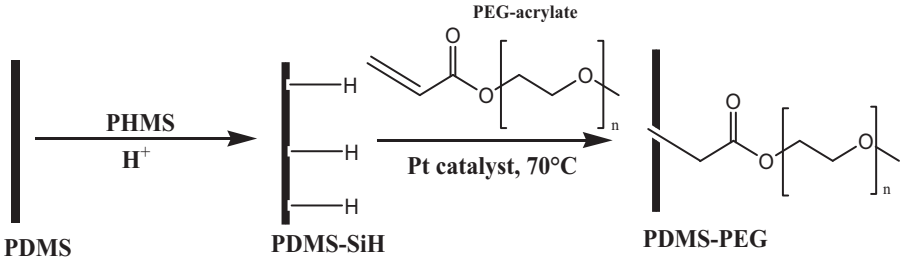

Fig. 1. Schematic of surface modification of PDMS.

(depending on the size of the plates and the instrument, values between 0.6 and 1×10^{-2} rad/N m were obtained for these systems) show that G' should be underestimated by 10–15% maximum. Due to the fact that small plates were used and that new rheometers are actually stiffer (MCR-501 from Anton Paar was estimated 2.5 times stiffer than the ARES), the compliance effect probably leads to an underestimate due to compliance effects of less than 5% on the elastic modulus of the samples.

2.2.5. Contact angle

In order to study the effect of surface modification on surface energy, static and dynamic contact angle experiments were performed using Krüss drop analysis system DSA30S (Krüss, Germany) for all the samples immediately after chemical modification. The static measurement was performed by creating a water drop of known volume (5 μL) at the tip of syringe needle, which was then gently brought into contact with the PDMS surfaces. The needle was then pulled back of the drop. A digital image was taken using a camera and analyzed by ImageJ software. For each sample, the contact angle was calculated by averaging the two contact angles of the droplets, for at least three droplets placed at different locations on the same PDMS surface.

Because static contact angle is not an equilibrium measurement and relied heavily on the testing procedure, advancing and receding contact angles were also measured by increasing (growing phase) and then decreasing (contracting phase) of the drop volume to ensure that the three phase boundary line moved sufficiently over the surface 6 ± 5 μL. The contact angle of the drop in the growing state that reached a steady-state value was defined as the advancing contact angle. The lowest contact angle, occurring at the moment when the contact line started to move, is defined as the receding contact angle. The images of the drop were recorded and analyzed by ImageJ software. All measurements were performed in ambient air at room temperature.

2.2.6. JKR measurements

The experimental apparatus used, based on the Johnson-Kendall-Roberts (JKR) theory of adhesive contact between elastic bodies, is described in details in [43]. It consists in a hemispherical unmodified PDMS lens with a diameter of 2.24 mm and a flat modified or unmodified PDMS sheet sample placed on two holders. To avoid finite size effects in the sphere reported in [44], a thick sheet of the same PDMS is intercalated between the sphere and the holder. The PDMS lens can be adjusted in the x, y, and z directions. A video camera connected to a microscope records the evolution of the contact radius a as a function of the applied load F. All data points were gathered every 5 min (for the unmodified PDMS) or 30 min (for the modified PDMS) to allow for viscoelastic relaxation in the PDMS. Two loading–unloading cycles at different depths were performed. Only loading data will be presented in this study since they give access to the thermodynamical work of adhesion between the surfaces, and thus a direct comparison with the Young–Dupré equation. On the contrary, complex phenomena occur during the unloading phase (due to dangling chains or unreacted species) and can have a significant impact on the measured energy [45].

Table 1
ATR-FTIR characteristic bands of unmodified and modified PDMS.

Group	Vibration type	IR region (cm^{-1})
Si—O—Si	Stretching vibration	1100–1000 cm^{-1}
Si—CH_3	Stretching vibration	1275–1245 cm^{-1}, 865–750 cm^{-1}
CH_2	Bending vibration (Si—CH=CH_2)	1410 cm^{-1}
C—H	Stretching vibration (CH_3 and CH_2—O)	3000–2850 cm^{-1}
Si—H	Stretching vibration	2300–2100 cm^{-1}
C=O	Stretching vibration	1740–1680 cm^{-1}
OH	Stretching vibration	3500–3200 cm^{-1}

3. Results and discussion

3.1. ATR-FTIR

The main characteristic bands of unmodified and modified PDMS in the 500–4000 cm^{-1} region are shown in Table 1 [46].

The unmodified PDMS spectrum displays the typical bands revealing the backbone structure of the network —$Si(CH_3)_2$—O—. All these peaks can also been identified for both modified PDMS (see Fig. 2a).

A worth noting point is that a small peak at 1598 cm^{-1} (Fig. 2b) can clearly be seen in the spectrum for the unmodified PDMS, and is also present with a small shift for the modified samples (1612 cm^{-1} for the PDMS–SiH and 1642 cm^{-1} for the PEG-modified PDMS), which could be assigned to the stretching vibration of C=C bonds and indicate that some terminal vinyl groups did not react during the crosslinking reaction (this can be confirmed by ^{1}H NMR of a Sylgard 184 mixture of base and curing agent in a 10:1 ratio, showing an excess of vinyl groups over Si—H functions, data not shown).

Fig. 2b zooms in the region of interest concerning the peaks concerning the modifications induced by the two-step procedure. In particular, the major difference among these spectra is the appearance of a strong new band of Si—H at 2166 cm^{-1} on the PDMS–SiH surface, which is not present on either the unmodified PDMS surface or the PEG-modified PDMS surface, making it an easy way to follow PEG modification. Following hydrosilylation, the appearance of a new broader CH_2 stretching vibration around 2870 cm^{-1} corresponds to the CH_2—O repeat group in the PEG-modified surface. This peak is not present on either the unmodified surface or on the PDMS–SiH surface. In addition, another peak appears at 1742 cm^{-1} on the PEG-modified surface. This peak is assigned to the PEG-acrylate carbonyl group (at one end of PEG-acrylate). Considering that free PEG-acrylate has been removed to form PDMS–PEG, the ATR-FTIR results clearly demonstrate that PEG chains have been covalently linked to the PDMS network by 1,2-addition hydrosilylation reaction. One should also note the presence of a small broad

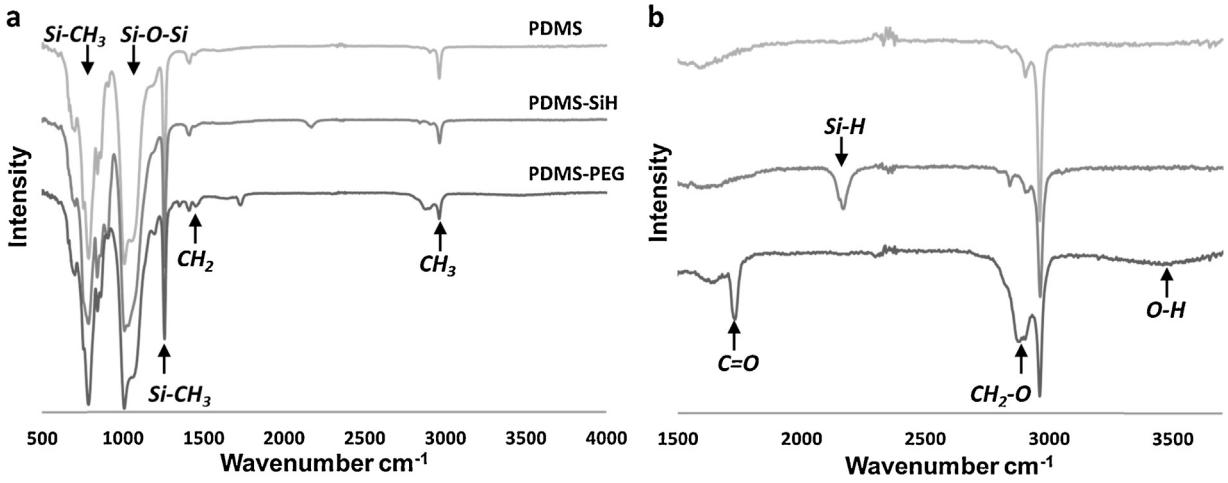

Fig. 2. ATR-FTIR spectra for control PDMS (light gray), PDMS–SiH (gray) and PDMS–PEG (dark gray) (a), with assignment of chemical functions present in the 3 samples. Zoom in the 1500–3700 cm^{-1} region (same color code) (b), with assignment of specific chemical functions due to the chemical modifications.

peak at 3500 cm^{-1} in the PEG-modified PDMS sample. This could reveal the presence of Si—OH resulting from the hydrolysis of some SiH groups. However, the high frequency of the peak (typical value for Si—OH is 3400–3200 cm^{-1}) probably rather reveals the presence of water, due to the hydrophilicity of the PEG-surface.

Finally, let us point out that the depth of penetration of the ATR-FTIR, on the order of 1 μm, and the intensity of the characteristic peaks for the modifications, suggest that the chemical reactions may occur not only on the surface but also within some depth of the sample. This can be explained by the fact that though methanol and diethylene-glycol dimethyl ether are poor solvent for PDMS, they can still swell the network by a small amount and thus lead to chemical reaction within the network near the surface [47].

3.2. Surface characterization by AFM

Fig. 3 shows pictures of whole samples deposited on top of a grid, and AFM images of the PDMS and PEG-modified PDMS surfaces under different modification times. It is clear from the top pictures that the samples lose some transparency when modified (the grid below becomes less and less visible), with a more pronounced effect when the modification time is increased, even though they all remain translucent. AFM image of the surface shows an almost perfectly flat surface for the unmodified PDMS ($R_q \sim 1$ nm). Similar to the unmodified PDMS, the roughness of the PDMS–SiH is found to be 2 nm (image not shown). This result indicates that the incorporation of SiH groups on the PDMS surfaces using acid catalysis does not affect the surface roughness and that, for these reaction times (30 nm for this first step), the acid does not significantly depolymerizes the PDMS (or, if so, in a uniform manner at the lateral resolution of the AFM).

However, the morphology of the PEG-modified PDMS surface is clearly impacted by the PEG grafting step. After 4 h of modification, the PEG-modified PDMS displays a rougher surface than the unmodified PDMS ($R_q \approx 10$ nm). Actually, the surface is mostly flat with aggregates having diameters (or lateral sizes) of few hundreds of nm and height around 50 nm. After 15 h of modification, the roughness remains similar ($R_q \approx 15$ nm, image not shown). However, for 24 and 48 h of modification, the roughness increases sharply (around 100 nm for 24 h and up to 200 nm for 48 h). The aggregates increase both in heights and lateral dimensions (up to a few microns). The appearance and growth of these regions as modification time increases can explain the loss in transparency. Similar morphologies on PEG-modified PDMS have been observed [36,37] and explained by a phenomenon of phase separation between PEG and PDMS due to the incompatibility between the two polymers. However, in these systems, PEG was added in default and not in excess, and the resulting height of the patterns was only a few nm. The height of the patterns measured here is much higher than the size of the very short PEG chains, and so the aggregation mechanism remains unclear since the samples are thoroughly washed before testing using a good solvent for short PEG chains (acetone). The increase in roughness could also be the result of the migration to the surface, due to the chemical modifications, of some of the thin polymer layers covering silica and other reinforcing fillers present in the Sylgard 184, as suggested by Genzer et al. [48].

3.3. Rheology

Rheological measurements performed on different PDMS samples show the influence of the chemical modification on the viscoelastic properties of the materials. In Fig. 4, deformation sweep measurements are presented (G', left, G'', right).

First, one can notice that all the materials shown here are very elastic ($G' \sim 10G''$) in all the deformation range. It is also noticeable that the results are fairly reproducible: concerning the unmodified 1:10 PDMS cured 17 h at 70 °C, 7 samples were tested using the same procedure. The standard deviation was below 8% for every data point for the G'.

Then, using a Poisson's ratio of 0.5 for PDMS [49], one can estimate the Young's modulus for the unmodified 1:10 PDMS as measured by this technique. This leads to a value close to 0.85 MPa in all the deformation range ($G' \sim 0.275$ MPa). This value is quite substantially lower than what is usually reported for PDMS prepared under similar conditions and measured with different techniques. For example, using rheological experiments with samples crosslinked in situ, Nase et al. [13] obtained a value of 2.4 MPa for a 1:9 PDMS cured at 80 °C for 5 h under vacuum, and 0.87 MPa for a 1:15 sample prepared under the same conditions. Using JKR, Poulard et al. [10] obtain a value of 1.8 MPa for a 10:1 sample cured at 50 °C during 24 h, while using the same technique, Davis et al. obtain a value of 2 MPa for a sample cured at 70 °C for 24 h [50].

However, such discrepancies between different techniques have already been reported concerning measurements of PDMS moduli [51]. In this article, nanoindentation, DMA, JKR and rheological measurements were used to measure the elastic modulus of 1:10 PDMS samples cured 4 h under vacuum at 65 °C. A value close to 1 MPa was obtained via rheology (0.1–10 Hz, 0.1% strain) while JKR value was close to 2 MPa (DMA was in between, and nanoindentation even higher, close to 3 MPa). The reasons for these

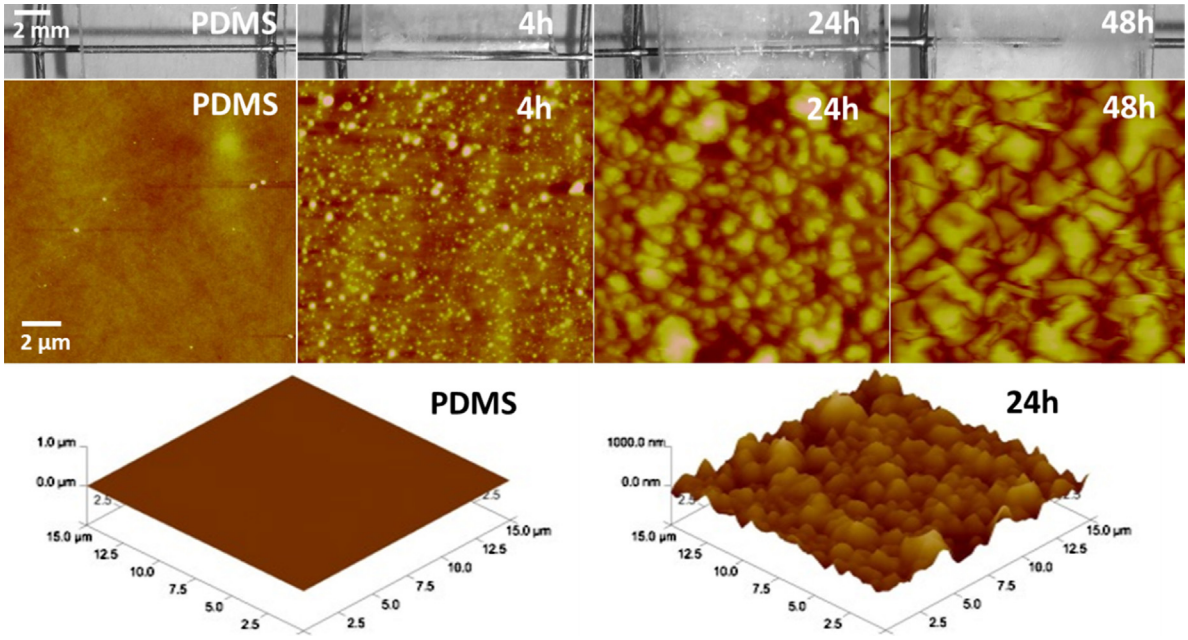

Fig. 3. Top row: Pictures of unmodified PDMS and PEG-modified PDMS samples with different modification times. Middle row: AFM surface topographies of unmodified and PEG-modified PDMS with different modification times. Bottom row: 3D images of the unmodified PDMS and PEG-modified PDMS with 24 h of modification time.

discrepancies have not been discussed in details, but it appears that compliance effects in that case could not explain the amount of the variations, even though the modulus showed in Fig. 3 might be underestimated by 10% (see materials section).

Since reproducibility of the experiment remain satisfactory, if we compare G' of the unmodified PDMS to the value of the PEG-modified 1:10 PDMS (24 h modification), G' for these samples is 0.35 MPa, a 25% increase. One could assume that this increase in the shear modulus is due to the extra-curing time induced by the modification if unreacted species remain in the sample, because the reaction is performed also at 70 °C for 24 h right after the 17 h curing. Indeed, the 41 h (e.g. 17 + 24 h) cured PDMS has a G' value of 0.3 MPa slightly above the 17 h cured PDMS (which demonstrates that little crosslinking occurs spontaneously in the sample after the first 17 h of curing). However, G' is still roughly 15% below G' of the PEG-modified PDMS.

This small difference between the 41 h cured PDMS and the PEG-modified one may then be explained by the chemical reaction adding new SiH functions in the material which will react on the surface with the PEG, but can also react with the remaining double bonds (as shown in Section 3.1) and cause a small extra-crosslinking over some depth within the sample.

However, if one wants, for example, to compare modified samples with unmodified ones having same viscoelastic properties in terms of adhesive of wetting properties, this rather slight increase can be easily addressed: a 1:9 PDMS cured for 17 or 41 h (data not shown) has a G' of 0.335 MPa, remarkably close to the one measured for the PEG-modified 1:10 PDMS.

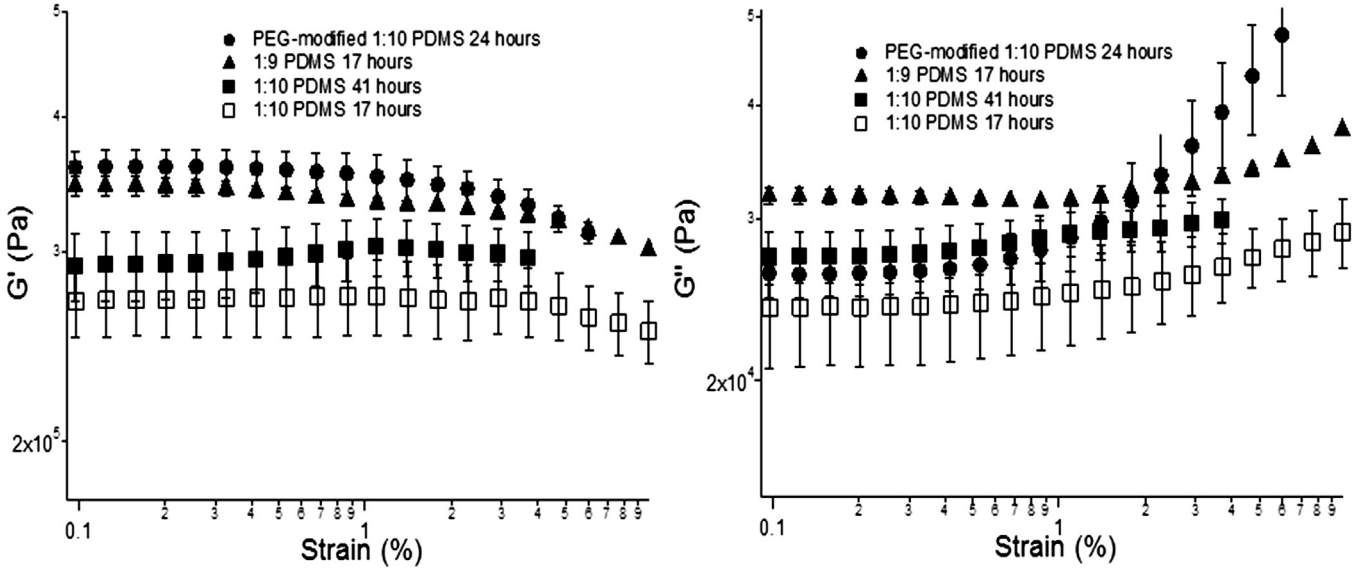

Fig. 4. Storage modulus G' (left) and loss modulus G'' (right) as a function of strain at constant frequency (1 Hz) for modified and unmodified PDMS at different curing times and curing agent ratio. The data points are the average over all the samples tests (see Section 2), the error bars represent the standard deviation from this average values calculated for each point.

Values for G'' are all comparable for every samples tested (between 25 kPa and 32 kPa below 2% deformation). The slight increase at higher strains may reveal slippage during the test or an increase in the viscoelasticity at higher deformations.

3.4. Water contact angle

In this study, water contact angle measurements are performed to assess the hydrophobicity of the surfaces before and after modification with PEG-acrylate. The contact angle values measured immediately after the chemical treatment for the various samples are presented in Fig. 5.

As expected, the unmodified PDMS is found to be strongly hydrophobic, with a static angle of about 110°, consistent with many results presented in the literature [52]. However, modification of PDMS with PEG-acrylate has a significant impact on the measured water contact angle. Its value decreases at first with modification time. After 24 h of reaction, static contact angle reaches a value of $67° \pm 2$.

For higher modification times (48 and 72 h), the value of the contact angle modified PDMS then reaches a plateau value ($65° \pm 2$). The sharp decrease in the contact angle from 80° to 67° when modification time increases from 15 to 24 h may be correlated to the increase in surface roughness induced by the density of PEG grafting as discussed above. This contact angle shift with the PDMS–PEG confirms again the existence of PEG on the surface. These values are greater than that of pure PEG films (20–25°) [53] and indicate either that the surface is not fully covered by PEG chains or that the water still partially "feels" the PDMS underneath the PEG layer, due to its thinness. The observed trends reflects the increase in chain density of PEG at the surface of the PDMS and probably indicates that for reaction times higher than 24 h, the concentration of grafted PEG at the surface is maximal. It is also worth noting that a synthesis conducted for 24 h with a doubled concentration of PEG-acrylate during the reaction step also leads to a value of 67° for the static contact angle. This confirms the excess of PEG-acrylate in the step 2 of the reaction, and that there is a limit in terms of grafting density of PEG on the PDMS surface.

In order to use these samples for example for adhesion tests, hydrophobic recovery in air of the chemically treated surface is also estimated by measuring the contact angle at regular intervals of time after the surface treatment. For example, the initial contact angle achieved immediately after the treatment of 72 h is 65° but subsequently increases to about 90° after about 4 weeks in air. This relatively slow increase in contact angle over time is in agreement with other reports [54] indicating that there is gradual hydrophobic recovery of the treated surface due to migration of low molecular weight species, from the bulk to the surface, or due to reorientation of the PEG hydrophilic groups away from the surface. However, storage of the samples in distilled water at room temperature allows the same contact angles to be measured over a two weeks period (data not shown).

To obtain further insights on the properties of PEG coated PDMS surface, dynamic contact angle measurements have been obtained by continuously enlarging and subsequently reducing the size of water drop through an embedded needle and recording the evolution of the contact angle over the radius of the droplet. Fig. 6 shows typical optical images of advancing, and receding water drops dynamic contact angle measurements on PDMS surface before and after 24 h of chemical modification. In the case of unmodified PDMS, the results of the contact angle measurements show that their mean advancing and receding contact angles are $\theta_a = 114° \pm 2$ and $\theta_r = 89° \pm 2$, respectively. The associated contact angle hysteresis is about 25°. Chemical modification with PEG has a significant effect on the advancing and receding contact angles which are about $83° \pm 2$ and $40° \pm 2$ respectively for PEG-modified PDMS for 24 h. The contact angle hysteresis is then 43°. It is seen that the PEG-modified PDMS showed a significant decrease in both advancing and receding contact angles for modification times below 24 h, but also a significant increase in the contact angle hysteresis. Though changes in crosslink densities (or Young's moduli) of elastomers can affect both contact angles and hysteresis [55,56], it is a fairly small effect when comparing samples with only a 25% difference in the modulus, and so it could not account for the significant differences measured in this study between unmodified and modified PDMS. However, this may indicate PEG chains local movements toward the water during the experiment or confirms the effects due to chemical heterogeneity or surface roughness appearing after the chemical treatment [57]. The observed difference in the two angles could also be due to the surface penetration of water during contact angle determination. After 24 h of modification, PDMS surfaces show a constant advancing and receding contact angle with time which is consistent with the previous hypothesis that all silicone hydride bonds (Si—H) created on the surface have already reacted. It is worth noting that these values are similar reported values from the literature for PEG-modified PDMS surfaces [33,37].

3.5. JKR

The JKR test allows a direct estimation of the work of adhesion (W) and the elastic modulus (E) of two elastic bodies in contact by the simultaneous measurement of applied load (F) and the radius of the contact area (a) at the interface under equilibrium conditions [58]. For the case of an elastic hemisphere in contact with a flat substrate, Eq. (2) models the JKR contact mechanics (Eq. (3)):

$$\frac{F}{\sqrt{6\pi a^3}} = K\left(\frac{a^{3/2}}{\sqrt{6\pi}\cdot R}\right) - \sqrt{WK} \tag{3}$$

where R is the radius of curvature of PDMS lens, F is the applied load, K is the composite elastic constant of the system lens/substrate, W is the work of adhesion.

When the material of the sphere and of the flat substrate are the same, the Young's modulus, E, can be calculated from the elastic constant, K, and the Poisson ratio, ν (Eq. (4)):

$$K = \frac{2}{3} \times \frac{E}{1-\nu^2} \tag{4}$$

The work of adhesion between two solids 1 and 2 can be estimated from the interfacial energies by the Young–Dupré equation (Eq. (5)):

$$W = \gamma_1 + \gamma_2 - \gamma_{12} \tag{5}$$

where γ_1, γ_2, and γ_{12} are respectively the surface free energy of solid 1, solid 2 and the interfacial energy of solid 1 in contact with solid 2, expressed in mJ/m^2.

In order to compare elastic modulus values obtained via the rheological experiments with those obtained using the JKR technique and gain information about the adhesive behavior of the samples, loading measurements using the JKR technique were performed, and are shown in Fig. 7 in the linearized form of Eq. (2), $F/\sqrt{6\pi a^3}$ being plotted as a function of $a^{3/2}/\sqrt{6\pi}R$. The experimental data are fitted with Eq. (3), then allowing measurements of W and K (and thus E).

By fitting the measured curve for two identical surfaces of 1:10 PDMS cured during 17 h to Eq. (2), the work of adhesion was found to be $W = 50\ mJ/m^2 \pm 3.6$. The corresponding measured surface energy is then $\gamma_1 = \gamma_2 = 25\ mJ/m^2$ (since in this case $\gamma_{12} = 0$), in agreement with previous studies [14]. The elastic modulus obtained from the fit is 1.45 MPa. For 1:10 PDMS samples cured during 41 h, the fit between the experimental loading data and Eq. (2) yielded values: $W = 50\ mJ/m^2 \pm 1.6$ (hence same surface energy)

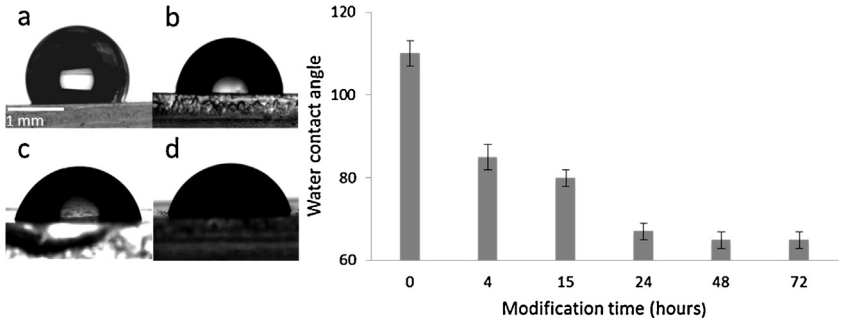

Fig. 5. Left: Water contact angle for (a) native PDMS; (b) PEG-modified PDMS after 4 h; (c) PEG-modified PDMS after 24 h and (d) PEG-modified PDMS after 72 h. Right: water contact angles for modified PDMS with different reaction times.

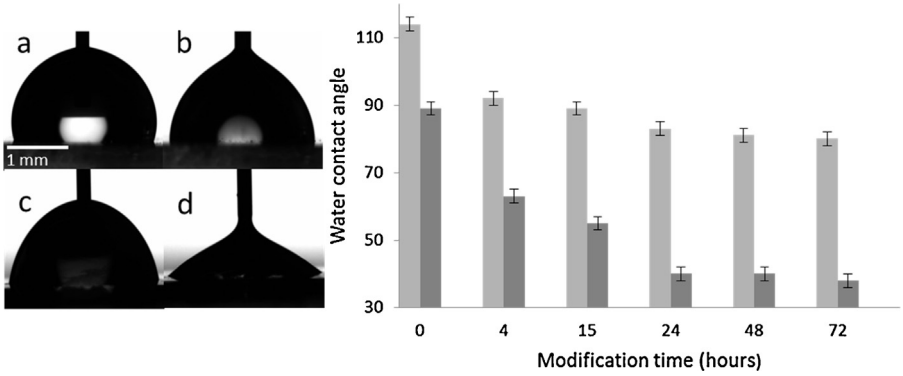

Fig. 6. Left: Typical optical images for advancing (a) and receding contact angle (b) of water for unmodified PDMS. (c) and (d) are respectively the advancing and the receding contact angle contact angle of PEG-modified PDMS after 24 h of treatment. Right: Advancing (light gray bars) and receding (dark gray bars) water contact angles for modified PDMS with different reaction times.

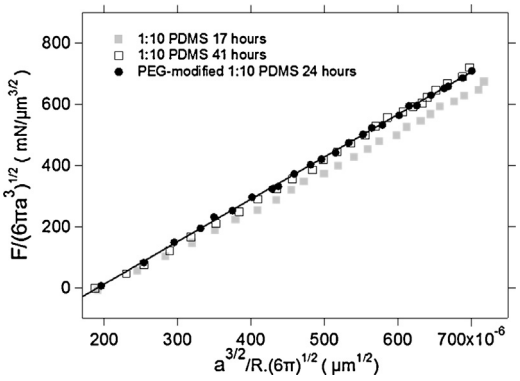

Fig. 7. Curves showing the behavior of PDMS samples (semispherical unmodified PDMS lens on flat sheet) of 1:10 PDMS cured 17 h at 70 °C (full gray square), 1:10 PDMS cured 41 h (open square) and PEG-modified PDMS with 24 h of reaction time (black circle) during loading cycle.

and $E = 1.65$ MPa, showing a small increase in Young modulus as already observed with the rheological measurements.

Using the same unmodified PDMS lens for the measurements but now in contact with a 24 h PEG-modified 1:10 PDMS substrate, we obtain $W = 52$ mJ/m^2 ± 2.7 and $E = 1.74$ MPa.

First, it is worth noting that there is a difference between the elastic modulus measured by JKR and by rheology, similar to what other researcher groups [51] have observed for similar material systems using different measurements techniques, as discussed above. Still, the differences observed for unmodified and modified PDMS are consistent for the two techniques (around 20% increase in the modulus for the modified PDMS over the unmodified one cured for 17 h, and 10% over the 41 h cured sample). Furthermore, the values obtained from the JKR test are in agreement with the ones reported by other studies [10,41].

Second, a small change in work of adhesion is observed between identical and modified substrates. This may appear surprising, as the surface free energy of the modified substrate should be larger than that of unmodified PDMS, as suggested by the contact angle measurements. However the analysis of the JKR result has to be done carefully due to the asymmetric nature of the contact, which thus implies a non-zero interfacial energy γ_{12}. To try to estimate the surface energy of the PEG-modified PDMS (γ_2), we use $\gamma_1 = \gamma_{PDMS} = 25$ mJ/m^2 and roughly estimate γ_{12} (PDMS surface and PEG-modified PDMS surface) by $\gamma_{PEG\text{-}PDMS}$.

The latter can be measured by using Young equation for a drop of PEG resting on an unmodified PDMS substrate (Eq. (6)):

$$\gamma_{PDMS} - \gamma_{PEG} * \cos\theta = \gamma_{PEG\text{-}PDMS} \quad (6)$$

where θ is the equilibrium contact angle of the drop on the substrate.

Using the procedure described in Section 2.2.5, the advancing contact angle between PDMS and PEG-acrylate has been measured at 61.6° ± 1.3 and the receding contact angle at 45° ± 2. The equilibrium contact angle in Young equation has been defined as $(1/2)(\theta_a + \theta_r)$ by Brochard-Wyart et al. [59], which gives 53.3° here. A more complicated analytical expression has been proposed by Tadmor [60] and leads to 55° with our measurements. The surface energy of PEG γ_{PEG} is reported to be 42–45 mJ/m^2 for high molecular weights [49]. However, molecular-weight dependence has been predicted for surface tension of polymers and observed experimentally for many polymers, such as PEG with various end groups, in the low molecular weight (oligomeric) range [61]. For $M_n = 480$ g/mol, the surface energy for PEG can be estimated at $\gamma_{PEG} \sim 37$–39 mJ/m^2 (using both experimental data for similar molar masses listed in Ref. [49] and empirical equations in Ref. [61]).

This finally leads to an estimated value of $\gamma_{PEG\text{-}PDMS} \sim 2\text{–}3\ mJ/m^2$. Then, according to Eq. (4), the corresponding surface energy of PEG modified 1:10 PDMS is 29–30 mJ/m^2. This value represents an increase of 20% relative to that of unmodified PDMS, even if still below the surface energy of PEG. This may reflect the fact that the grafted PEG chains are short (the PEG molecule used is about 9 or 10 monomeric units), which means PDMS is still "seen" macroscopically when surfaces are in contact, but could also mean that the surface is not fully covered by PEG chains.

One could state that the adhesion energy can also be affected by the roughness of the surfaces. Unfortunately only little is known of the exact role of roughness on the adhesion energy extracted from a JKR test since it is always difficult to guarantee that the surface topography and not the chemistry have been changed. Nevertheless, a paper by Verneuil et al. showed that when the roughness is small (typically smaller than 200 nm) as is the case in this study, its effect on the thermodynamical work of adhesion is small. Moreover, this roughness effect leads to a decrease in the work of adhesion, which would mean an underestimated value for the surface energy of the PEG-modified PDMS [62].

Anyhow, one should not over-interpret the values presented above. Indeed, we would like to point out that this estimate, which is in agreement with the contact angle experimental results, remains semi-quantitative due to the fact that the effect is quite small, and to cumulative uncertainties on both the JKR experiments and fits, the definition of an equilibrium contact angle when hysteresis is present, the effect of roughness, and the available reported values of surface tensions.

4. Conclusion

The surface modification of PDMS surfaces with PEG-acrylate has been successfully achieved using a two-step technique and leads to a significant increase in surface hydrophilicity. Compared to unmodified PDMS, PEG-modified exhibited lower water contact angle (down to 65° for the static contact angle) and a significant increase in the hysteresis. It is shown that this reaction can be made without impacting significantly the viscoelastic properties (G' and G'') of the PDMS but with a slight effect on the surface roughness ($\sim$100 nm).

The surface energy of PEG-modified PDMS has been measured close to 30 mJ/m^2 compared with 25 mJ/m^2 for the unmodified PDMS, which is in semi-quantitative agreement with the contact angle results.

To clarify the role of chemical interactions at the interface and surface patterning as well as viscoelasticity effects on adhesion, friction and wetting, further work will deal with the transfer of the described two-step technique for the modification of PDMS surfaces presenting controlled micron-sized patterns (such as wrinkles, lines or posts) to tune independently both surface patterning and surface chemistry of the PDMS, while the viscoelastic properties of the PDMS can simply be changed by varying the amount of crosslinker. The combination of fabricating a patterned structure and a tailored chemistry surfaces without changing its original structure and rheological properties would non-only increase our understanding in the coupling between topography and surface chemistry in the surface properties of materials, but also open up opportunities for new adhesive materials with well-designed surfaces.

Acknowledgments

Dr. Laurent Bouteiller and Prof. Eric Drockenmuller are gratefully acknowledged for fruitful discussions concerning the chemical modifications and Prof. G.B. McKenna for his insight on the rheological tests and for providing helpful references. The authors would also like to thank Dr. Sebastien Roland for his help with the AFM measurements and Dr. Matthieu Gervais for his help with the ATR-FTIR analysis. The authors would finally like to acknowledge financial support from the Agence Nationale de la Recherche (ANR) grant number ANR-11-BS04-0030 [WAFPI].

References

[1] R.K. Shull, Contact mechanics and the adhesion of soft solids, Mater. Sci. Eng. R 36 (2002) 1–45.
[2] A. Jagota, S.J. Bennison, Mechanics of adhesion through a fibrillar microstructure, Integr. Comp. Biol. 42 (2002) 1140–1145.
[3] A.J. Crosby, M. Hageman, A. Duncan, Controlling polymer adhesion with "pancakes", Langmuir 21 (2005) 11738–11743.
[4] C. Greiner, A. Del Campo, E. Arzt, Adhesion of bioinspired micropatterned surfaces: effects of pillar radius, aspect ratio, and preload, Langmuir 23 (2007) 3495–3502.
[5] D.E. Packham, Surface energy, surface topography and adhesion, Int. J. Adhes. Adhes. 23 (2003) 437–448.
[6] S.K. Thanawala, M.K. Chaudhury, Surface modification of silicone elastomer using perfluorinated ether, Langmuir 16 (2000) 1256–1260.
[7] B.N.J. Persson, O. Albohr, U. Tartaglino, A.I. Volokitin, E. Tosatti, On the nature of surface roughness with application to contact mechanics, sealing, rubber friction and adhesion, J. Phys.: Condens. Matter 17 (2005) R1–R62.
[8] M. Barquins, M.E.R. Shanahan, Effect of surface cavities on static and dynamic adhesion to an elastomer, Int. J. Adhes. Adhes. 17 (1997) 313–317.
[9] R. Elleuch, K. Elleuch, H. Ben Abdelounis, H. Zahouani, Surface roughness effect on friction behaviour of elastomeric material, Mater. Sci. Eng. A 465 (2007) 8–12.
[10] C. Poulard, F. Restagno, R. Weil, L. Léger, Mechanical tuning of adhesion through micro-patterning of elastic surfaces, Soft Matter 7 (2011) 2543–2551.
[11] E. Degrandi-Contraires, C. Poulard, F. Restagno, L. Léger, Sliding friction at soft micropatterned elastomer interfaces, Faraday Discuss. 156 (2012) 255–265.
[12] M.E.R. Shanahan, F. Michel, Physical adhesion of rubber to glass: cross-link density effects near equilibrium, Int. J. Adhes. Adhes. 11 (1991) 170–176.
[13] J. Nase, O. Ramos, C. Creton, A. Lindner, Debonding energy of PDMS a new analysis of a classic adhesion scenario, Eur. Phys. J. E 36 (2013) 103.
[14] M.K. Chaudhury, G.M. Whitesides, Direct measurement of interfacial interactions between hemispherical lenses and flat sheets of poly(dimethylsiloxane) and their chemical derivatives, Langmuir 7 (1991) 1013–1025.
[15] X. Ren, M. Bachman, C. Sims, G.P. Li, N. Allbritton, Electroosmotic properties of microfluidic channels composed of poly(dimethylsiloxane), J. Chromatogr. B: Biomed. Sci. Appl. 762 (2001) 117–125.
[16] S.L. Peterson, A. McDonald, P.L. Gourley, D.Y. Sasaki, Poly(dimethylsiloxane) thin films as biocompatible coatings for microfluidic devices: cell culture and flow studies with glial cells, J. Biomed. Mater. Res. Part A 72 (2005) 10–18.
[17] H. Hillborg, J.F. Ankner, U.W. Gedde, G.D. Smith, H.K. Yasuda, K. Wikstro, Crosslinked polydimethylsiloxane exposed to oxygen plasma studied by neutron reflectometry and other surface specific techniques, Polymer 41 (2000) 6851–6863.
[18] J. Kim, M.K. Chaudhury, M.J. Owen, T. Orbeck, The mechanisms of hydrophobic recovery of polydimethylsiloxane elastomers exposed to partial electrical discharges, J. Colloid Interface Sci. 244 (2001) 200–207.
[19] H. Hillborg, N. Tomczak, A. Olah, H. Schonherr, G.J. Vancso, Nanoscale hydrophobic recovery: a chemical force microscopy study of UV/ozone-treated cross-linked poly(dimethylsiloxane), Langmuir 20 (2004) 785–794.
[20] J.A. Vickers, M.M. Caulum, C.S. Henry, Generation of hydrophilic poly(dimethylsiloxane) for high-performance microchip electrophoresis, Anal. Chem. 78 (2006) 7446–7452.
[21] B. Schnyder, T. Lippert, R. Kotz, A. Wokaun, V.M. Graubner, O. Nuyken, UV-irradiation induced modification of PDMS films investigated by XPS and spectroscopic ellipsometry, Surf. Sci. 1067 (2003) 532–535.
[22] E.A. Waddell, S. Shreeves, H. Carrell, C. Perry, B.A. Reid, J. McKee, Surface modification of Sylgard 184 polydimethylsiloxane by 254 nm excimer radiation and characterization by contact angle goniometry, infrared spectroscopy, atomic force and scanning electron microscopy, Appl. Surf. Sci. 254 (2008) 5314–5318.
[23] H.Y. Chen, J. Lahann, Fabrication of discontinuous surface patterns within microfluidic channels using photodefinable vapor-based polymer coatings, Anal. Chem. 77 (2005) 6909–6914.
[24] H. Makamba, Y.Y. Hsieh, W.C. Sung, S.H. Chen, Stable permanently hydrophilic protein-resistant thin-film coatings on poly(dimethylsiloxane) substrates by electrostatic self-assembly and chemical cross-linking, Anal. Chem. 77 (2005) 3971–3978.
[25] J.D. Qiu, P.F. Hu, R.P. Liang, Separation and simultaneous determination of uric acid and ascorbic acid on a dynamically modified poly(dimethylsiloxane) microchip, Anal. Sci. 23 (2007) 1409–1414.
[26] G.T. Roman, T. Hlaus, K.J. Bass, T.G. Seelhammer, C.T. Culbertson, Sol–gel modified poly(dimethylsiloxane) microfluidic devices with high electroosmotic mobilities and hydrophilic channel wall characteristics, Anal. Chem. 77 (2005) 1414–1422.

[27] B.E. Slentz, N.A. Penner, E. Lugowska, F. Regnier, Nanoliter capillary electrochromatography columns based on collocated monolithic support structures molded in poly(dimethylsiloxane), Electrophoresis 22 (2001) 3736–3743.
[28] B.F. Liu, M. Ozaki, H. Hisamoto, Q.M. Luo, Y. Utsumi, T. Hattori, S. Terabe, Microfluidic chip toward cellular ATP and ATP-conjugated metabolic analysis with bioluminescence detection, Anal. Chem. 77 (2005) 573–578.
[29] G.T. Roman, S. Carroll, K. McDaniel, C.T. Culbertson, Micellar electrokinetic chromatography of fluorescently labeled proteins on poly(dimethylsiloxane)-based microchips, Electrophoresis 27 (2006) 2933–2939.
[30] Y. Luo, B. Huang, H. Wu, R.N. Zare, Controlling electroosmotic flow in poly(dimethylsiloxane) separation channels by means of prepolymer additives, Anal. Chem. 78 (2006) 4588–4592.
[31] J. Seo, L.P. Lee, Effects on wettability by surfactant accumulation/depletion in bulk polydimethylsiloxane (PDMS), Sens. Actuators B 119 (2006) 192–198.
[32] Z. Wu, W. Tong, W. Jiang, X. Liu, Y. Wang, H. Chen, Poly(N-vinylpyrrolidone)-modified poly(dimethylsiloxane) elastomers as anti-biofouling materials, Colloids Surf. B Biointerf. 96 (2012) 37–43.
[33] K. Yu, Y. Han, A stable PEO-tethered PDMS surface having controllable wetting property by a swelling–deswelling process, Soft Matter 2 (2006) 705–709.
[34] P. Gasteier, A. Reska, P. Schulte, J. Salber, A. Offenhausser, M. Moeller, et al., Surface grafting of PEO-based star-shaped molecules for bioanalytical and biomedical applications, Macromol. Biosci. 7 (8) (2007) 1010–1023.
[35] H. Chen, M.A. Brook, H.D. Sheardown, Y. Chen, B. Klenkler, Generic bioaffinity silicone surfaces, Bioconj. Chem. 17 (2006) 21–28.
[36] Y. Iwasaki, M. Takamiya, R. Iwata, S. Yusa, K. Akiyoshi, Surface modification with well-defined biocompatible triblock copolymers: improvement of biointerfacial phenomena on a poly(dimethylsiloxane) surface, Colloids Surf. B: Biointerf. 57 (2007) 226–236.
[37] H. Chen, M.A. Brook, H. Sheardown, Silicone elastomers for reduced protein adsorption, Biomaterials 25 (2004) 2273–2282.
[38] H. Chen, M.A. Brook, Y. Chen, H. Sheardown, Surface properties of PEO–silicone composites: reducing protein adsorption, J. Biomater. Sci. Polym. Ed. 16 (2005) 531–548.
[39] J. Nase, Debonding of Viscoelastic Materials: From a Viscous Liquid to a Soft Elastic Solid (Ph.D. thesis), Universitat des Saarlandes, Université Pierre et Marie Curie, 2009.
[40] F. Schneider, T. Fellner, J. Wilde, U. Wallrabe, Mechanical properties of silicones for MEMS, J. Micromech. Microeng. 18 (2008) 065008–065017.
[41] S.A. Hutcheson, Evaluation of Viscoelastic Materials: The Study of Nanosphere Embedment into Polymer Surfaces and Rheology of Simple Glass Formers using a Compliant Rheometer (Ph.D. thesis), Texas Tech University, 2008.
[42] S.A. Hutcheson, G.B. McKenna, The measurement of mechanical properties of glycerol, *m*-toluidine, and sucrose benzoate under consideration of corrected rheometer compliance: an in-depth study and review, J. Chem. Phys. 129 (2008) 074502–074516.
[43] M. Deruelle, H. Hervet, G. Jandeau, L. Léger, Some remarks on JKR experiments, J. Adhes. Sci. Technol. 12 (1998) 225–247.
[44] R.K. Shull, D. Ahn, L.C. Mowery, Finite-size corrections to the JKR technique for measuring adhesion: soft spherical caps adhering to flat, rigid surfaces, Langmuir 13 (1997) 1799–1804.
[45] P. Silberzan, S. Perutz, E.J. Kramer, Study of the self-adhesion hysteresis of a siloxane elastomer using the JKR method, Langmuir 10 (1994) 2466–2470.
[46] B. Arkles, et al. (Eds.), Silicon Compounds: Register and Review, Petrarch Systems, Bristol, PA, USA, 1987.
[47] J. Ng Lee, C. Park, G.M. Whitesides, Solvent compatibility of poly(dimethylsiloxane)-based microfluidic devices, Anal. Chem. 75 (2003) 6544–6554.
[48] K. Efimenko, J.A. Crowe, E. Manias, D.W. Schwark, D.A. Fischer, J. Genzer, Rapid formation of soft hydrophilic silicone elastomer surfaces, Polymer 46 (2005) 9329–9341.
[49] J.E. Mark (Ed.), Polymer Data Handbook, Oxford University Press, Oxford, UK, 1999.
[50] C.S. Davis, A.J. Crosby, Mechanics of wrinkled surface adhesion, Soft Matter 7 (2011) 5373–5381.
[51] C.C. White, M.R. Vanlandingham, P.L. Drzal, N.K. Chang, S.H. Chang, Viscoelastic characterization of polymers using instrumented indentation. II. Dynamic testing, J. Polym. Sci., Part B: Polym. Phys. 43 (2005) 1812–1824.
[52] T.Y. Chang, V.G. Yadav, S. De Leo, A. Mohedas, B. Rajalingam, C.-H. Chen, S. Selvarasah, R.M. Dokmeci, A. Khademhosseini, Cell and protein compatibility of Parylene-C surfaces, Langmuir 23 (2007) 11718–11725.
[53] P. Kim, D.H. Kim, B. Kim, S.K. Choi, S.H. Lee, A. Khademhosseini, R. Langer, K.Y. Suh, Fabrication of nanostructures of polyethylene glycol for applications to protein adsorption and cell adhesion, Nanotechnology 16 (2005) 2420–2426.
[54] D.T. Eddington, J.P. Puccinelli, D.J. Beebe, Thermal aging and reduced hydrophobic recovery of polydimethylsiloxane, Sens. Actuators B 114 (2006) 170–172.
[55] A. Carré, M.E.R. Shanahan, Effect of cross-linking on the dewetting of an elastomeric surface, J. Colloid Interface Sci. 191 (1997) 141–145.
[56] C.W. Extrand, Y. Kumagai, J. Colloid Interface Sci. 184 (1996) 191–200.
[57] Y.L. Chen, C.A. Helm, J.N. Israelachvili, Molecular mechanisms associated with adhesion and contact angle hysteresis of monolayer surfaces, J. Phys. Chem. 95 (1991) 10736–10747.
[58] K.L. Johnson, K. Kendall, A.D. Roberts, Surface energy and the contact of elastic solids, Proc. R. Soc. Lond., Ser. A 324 (1971) 301.
[59] C. Redon, F. Brochard-Wyart, F. Rondelez, Dynamics of dewetting, Phys. Rev. Lett. 66 (6) (1991) 715–718.
[60] R. Tadmor, Line energy and the relation between advancing, receding, and young contact angles, Langmuir 20 (2004) 7659–7664.
[61] S. Wu, Interfacial and surface tensions of polymers, J. Macromol. Sci., Part C 10 (1) (1974) 1–73.
[62] E. Verneuil, B. Ladoux, A. Buguin, P. Silberzan, Adhesion on microstructured surfaces, J. Adhes. 83 (2007) 449–472.